Journal of Sound and Vibration, Volume 469, March 2020, Article number 115134
DOI: 10.1016/j.jsv.2019.115134

A Novel approach for damage quantification using the dynamic response of a metallic beam under thermo-mechanical loads

Behzad Ahmed Zai[1], M. A. Khan[2], Kamran A. Khan[3], Asif Mansoor[4]

[1]*Department of Engineering Sciences, PN Engineering College, National University of Sciences and Technology (NUST), Karachi, Pakistan, behzad_zai@pnec.nust.edu.pk*
[2]*School of Aerospace, Transport and Manufacturing, Cranfield University, UK, muhammad.a.khan@cranfield.ac.uk*
[3]*Aerospace Engineering Department Khalifa University, Abu Dhabi, PO Box 127788, UAE, kamran.khan@ku.ac.ae*
[4]*Department of Engineering Sciences, PN Engineering College, National University of Sciences and Technology (NUST), Karachi, Pakistan, drasifmansure@pnec.nust.edu.pk*

Abstract: This paper investigates the interdependencies of crack depth and crack location on the dynamic response of a cantilever beam under thermo-mechanical loads. Temperature can influence the stiffness of the structure, thus, the change in stiffness can lead to variation in frequency, damping and amplitude response. These variations are used as key parameters to quantify damage of Aluminum 2024 specimen under thermo-mechanical loads. Experiments are performed on cantilever beams at non-heating (room temperature) and elevated temperature, i.e., 50°C, 100°C, 150°C and 200°C. This study considers a cantilever beam having various initially seeded crack depth and locations. The analytical, numerical and experimental results for all configurations are found in good agreement. Dynamic response formulation is presented experimentally on beam for the first time under thermo-mechanical loads. Using available experimental data, a novel tool is formulated for in-situ damage assessment in the metallic structures. This tool can quantify and locate damage using the dynamic response and temperature including the diagnosis of subsurface cracking. The obtained results demonstrate the possibility to diagnose the crack growth at any instant within the operational condition under thermo-mechanical loads.

Keywords: Crack depth, crack location, dynamic response, thermo-mechanical loads, crack prorogation.

1 Introduction

Mechanical properties of metallic structure are more often dependent on their operating temperature. Properties like Young's modulus, Yield strength or Ultimate tensile strength can change easily with varying temperature. In case of fatigue, failure is initiated from birth of a small crack and lead to catastrophic failure. The rise in temperature can lead to increase the size of the plastic zone near the crack tip which can affect crack propagation. Size of the plastic zone near the crack tip depends not only on the level of repeated loads but also on the material properties. It is very difficult to repair fatigue damage immediately. However, estimation of fatigue crack growth can make preventive maintenance much easier. Therefore, considering fatigue failure is the most common failure in mechanical structure, it is very critical to investigate the effect of thermal loads. There are many applications in which a structure undergoes combined dynamic and thermal loads such as aircraft wings, gas turbine blades and reciprocating pistons, etc. These components are more often exposed to extreme loads and raised significant challenges to ensure structural integrity. This significance propelled researchers in the past to investigate the potential of dynamic response parameters in damage quantification for structures working under thermo-mechanical loadings.

Conventional nondestructive testing techniques are used to measure local or global behavior of a structure for damage assessment [1]. Out of these techniques, structural vibration is used most rigorously for global response analysis and measurements [2]. It can identify specific faults in the system and can also lead the repair of structures or components by diagnosing the root cause of damage. Published methods show that a vibration response can estimate structural or component damage long before their potential catastrophic failure. This early warning of emerging damage helps in scheduling reliable preventive maintenance in any industry. The characteristic of vibration response, such as displacement amplitude, mode shape and frequency, is dependent on the stiffness of a structure. The stiffness of a structure is a direct measurement of elastic properties of its material [3]. The elastic properties of a material are determined by its microstructure and hence even a very small disturbance or damage in microstructure can eventually affect dynamic response of a system. Most of the research is done at ambient conditions based on mechanical loads only. Khorshidi et al. [4] proposed a natural frequency-based method to diagnose a transverse crack in a beam. The crack was modeled as massless rotational spring. They developed a relation between natural frequency and crack depth by using Rayleigh quotient. Similar approach of modeling a crack as massless rotational spring was adopted by few other researchers [5-7].

*Corresponding author: behzad_zai@pnec.nust.edu.pk
Mechanical Engineering, Pakistan Navy Engineering College,
National University of Science and Technology, Pakistan.
Cell phone: +923213789884,
ORICD: 0000-0002-2584-9006

New methods for damage quantification using natural frequency degradation are presented recently [8-10]. Their research is an excellent contribution to existing literature related to damage quantification. They proposed a novel explicit closed form solution of the governing equation of an Euler-Bernoulli beam with a roving body possessing mass and rotary inertia, in the presence of multiple cracks. Furthermore, they modeled concentrated damage as Dirac's delta distributions capturing the effect of concentrated stiffness reduction with the help of mode shape and natural frequencies. A significant number of researchers used analytical, numerical and experimental approaches simultaneously. They quantified crack in a beam and used natural frequency as an input [11-18]. They observed the changes in natural frequency if the crack propagates. Changes in natural frequency were found insignificant in case of smaller cracks and hence entailed modification in methods based on natural frequency. These frequency-based approaches are ill-posed because cracks with different severity in two sets of different locations can produce identical changes at lower frequency modes. The incorporation of mode shape with natural frequency provides better results in damage prediction but it has few limitations. It requires many sensors on a structure to capture the actual change in the physical shapes. These limitations can be circumvented with the measurement of vibration amplitude. Frequency and amplitude can be measured from a single probe and hence effective in use as compared to mode shape. [19-24].

Considering the coupled loading, Cheng et al. [25], used a thermal-acoustic load for testing dynamic response and sonic fatigue using Monte-Carlo theory. The effects of environmental conditions on modal behavior of different structures were presented by various researchers [26-30]. Ma et al. [31-32] proposed an analytical method (based on a transfer matrix) for modal analysis of a simply supported steel beam with multiple transverse open cracks under different temperatures. They modeled crack as a rotational spring and hence limited in damage quantification. Same approach was used by many other researchers [33-37] and they used change of natural frequency as critical input in the damage identification.

An algorithm for structure health monitoring was presented by many researchers [38-40]. They developed an integrated monitoring system for durability and assessment of bridges and turbine rotor at elevated temperatures. Their practice was mainly based on the response of different sensors and visual inspections using enhanced realistic deterioration models. Similar research overview is also presented in our recently submitted review paper [41].

Various researchers worked on fatigue under thermo-mechanical loads. However, still, efforts are required to develop a robust operative tool for damage assessment. Development of this tool requires focused research which can take in-situ response parameters as input to quantify damage. All the aforementioned research is limited to a specific structure and disparity of dynamic response due to temperature was estimated. Variation in response parameters due to damage was not covered. Therefore, a robust tool, equally applicable to other metallic structure can be very useful particularly for Aluminum 2024 which is a potential material used in aerospace applications.

This paper investigates the interdependencies of the structure's modal behavior, its dynamic response and crack growth based on analytical formulation, experimental data and empirical relations under thermo-mechanical loads. Dynamic response formulations are presented by Khorshidi [4] and Ostachowicz [6] for non-prismatic cantilever beam under dynamic loads only. Therefore, empirical correlations are formulated on a beam for the first time under thermomechanical loads to establish relation between dynamic response, temperature and crack parameters. In experimental validation, predicted crack growth obtained via these correlations is compared with the actual observations. A novel damage assessment tool is developed which takes frequency drop, amplitude difference, and temperature as an input to estimate damage during operational condition. This tool also covers the future of non-destructive testing by eliminating the requirement of contacting probes. Hence, it can be a useful contribution to the existing literature for damage assessment.

2 Specimen preparation

Aluminum (Al 2024) is the selected material of the specimen. All the dimensions of the particular shaped cantilever beam designed for dynamics response are shown in Figure 1. The thickness of the specimen is 3.0 mm and the length is 150 mm. These two dimensions are kept constant throughout the experiments for each specimen. Specimens with cracks have only one crack each. These cracks are induced on three different locations with respect to the length of the beam (i.e. Crack at 5% of total length, Crack at 10% of total length and Crack at 15% of total length). These locations are selected to get the maximum stress concentration at the fillet area of the specimen. Crack location is restricted to 15% of total length (25 mm from fixed end) because it is observed using a numerical simulation that after specific location of a crack from the fixed end the maximum stress concentration point moved from the crack position (desired location) to the fillet point. This shift in the location of stress concentration point will decrease the crack propagation rate to almost zero and lead to an endless motion of specimen without catastrophic failure.

A pre-defined crack is induced in each configuration with a constant width of 0.2 mm. The variation of crack depth ranges from 0.5 mm to 2.5 mm with an increment of 0.5 mm. The value of 0.5 mm shows that the crack is in its initial phase. Its maximum value goes up to 2.5 mm signifies the point where the crack has traveled to a value to cause catastrophic failure. The specimens are manufactured by CNC wire cut to maintain the required dimensional accuracy. Three different samples of each combination of crack depth and location are used to reduce experimental errors.

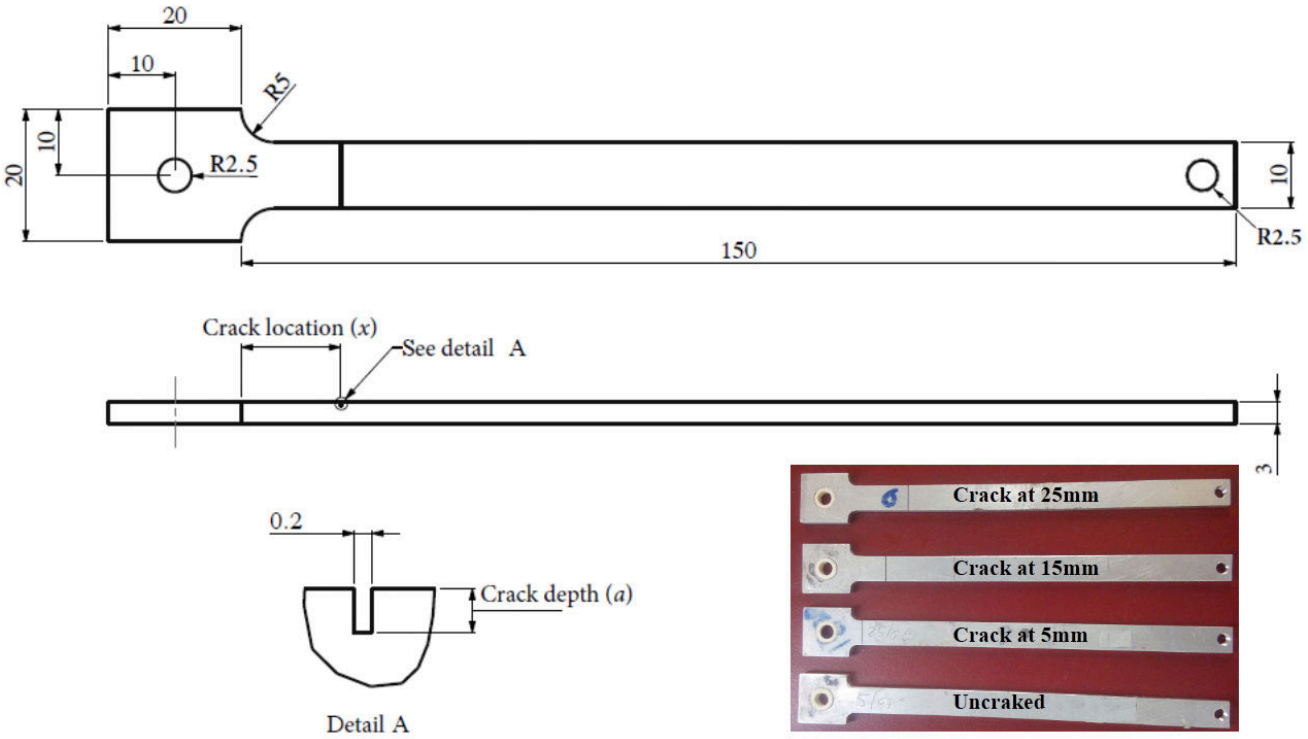

Figure 1: Dimensions of the specimen (in mm), inset is showing the manufactured specimen.

3 Experimental setup

There are two phases of experimentation. One covers the initially seeded cracks ranges from 0.5 mm to 2.5 mm with an increment of 0.5 mm. The other is with the initial crack of 0.5 mm with natural propagation under load. Each configuration is tested for five different temperatures: Non-heating (room temperature), 50°C, 100°C, 150°C, and 200°C. To avoid the possibility of recrystallization, the maximum temperature is chosen well below half of the melting point of aluminum 2024.

The whole experimental setup can be divided into four parts: a vibrating mechanism, a heating mechanism, data acquisition and propagation capture as shown in Figure 2. For the vibration mechanism, a power amplifier (modal LA-200), a signal generator (TENLEE 9200), and a modal exciter (MS-100) are used. The signal generator is used to provide a constant peak to peak value of 5 volts in a sine waveform, which consequently provides a constant displacement loading of ± 5 mm to the specimen with the help of the power amplifier. The beam specimens with pre-selected crack depth located at the same position are mounted on a modal exciter in fixed-free condition. An accelerometer is attached at the free end of the specimen to measure the dynamic response available in a frequency spectrum. The exciter and the specimen are firmly attached so any measured response can provide a cumulative amplitude of the dynamic response of the whole system which is largely dominated by the specimen displacement at the free end due to the resonance.

For the heating mechanism, a temperature control unit, cartridge heater and K-type thermocouple are used. A temperature control unit is used to control and monitor the required temperature. A small cartridge heater is installed at the end of the specimen to heat and maintain the required temperature. Insulation is placed between the specimen and the shaker to protect it from damage due to heat. The specimens are heated in an open environment, but the temperature in the testing lab is controlled with thermostat. Moreover, the specimens are heated continuously until the temperature difference between the thermocouple location and the free end is reduced and maintained within 10°C. Once the required temperature is achieved, then the mechanical loads are applied using shaker on a selected fundamental frequency.

Time domain measurements are obtained via a data acquisition card (NI-9174) and National Instrument© Signal Express. The analysis modules of 'Power Spectrum' and 'Amplitude and Levels' are selected in the Signal Express. The former is used to identify the actual response frequency value, while the latter is used to obtain the actual amplitude of the response frequency. The frequency drop is continuously observed. In the case of a frequency drop, the peak amplitude of the vibration spectrum is also reduced. A new lower frequency is set to the shaker so that the maximum amplitude can be achieved. A new fundamental frequency of the specimen is maintained till the next frequency drop. This procedure is repeated until the catastrophic failure of the specimen for propagating crack only. The failure of the specimen is defined as when it can no longer show amplitude at the free end. For each specimen, modal frequency and propagating crack depth are measured using a Dino-lite digital microscope with a magnification of 200x. Detailed experimental scheme for initially seeded and propagating crack is shown in Figure 3.

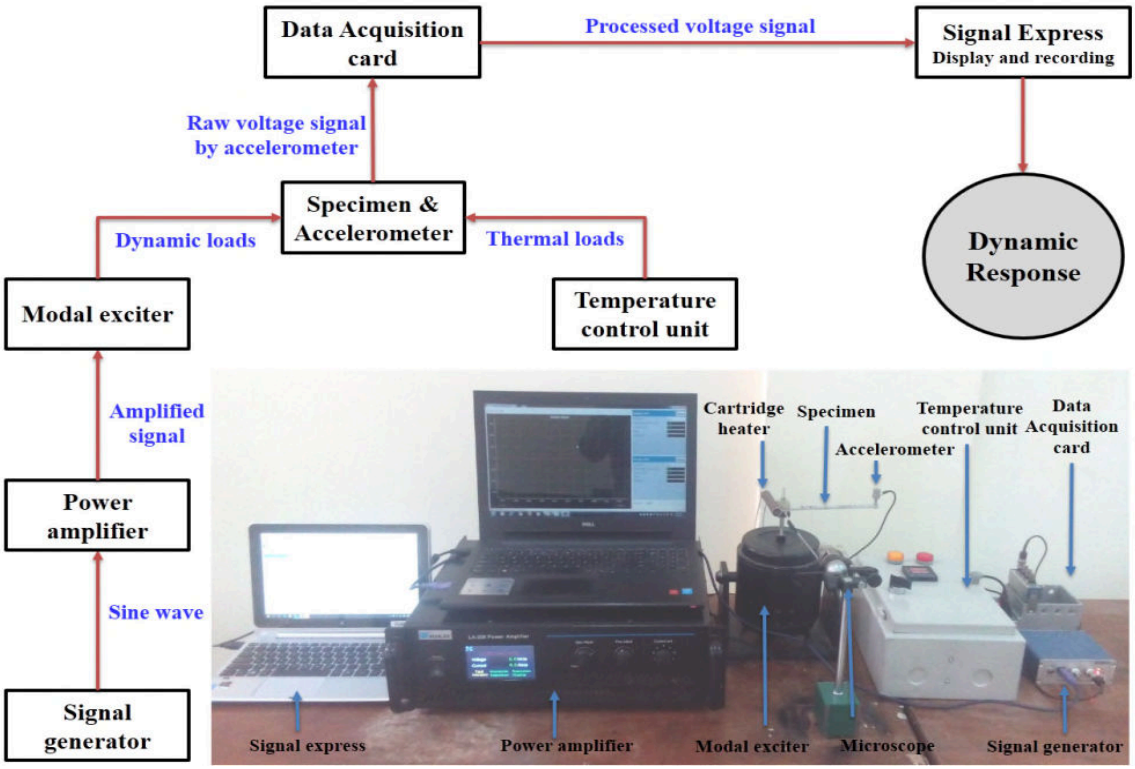

Figure 2: Experimental setup with schematic.

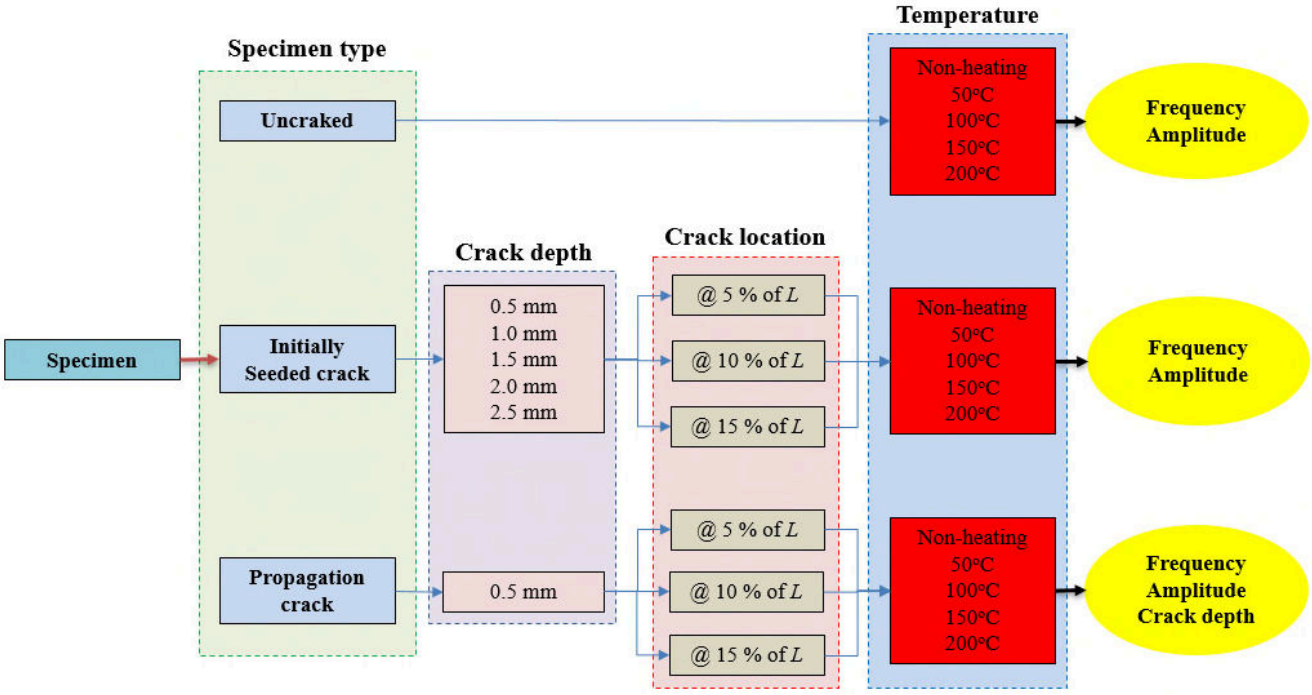

Figure 3: Detailed experimental scheme

4 Methodology

4.1 Analytical formulation under thermo-mechanical loads

In this section, an analytical formulation is presented which describes the effect of crack depth in terms of stiffness reduction of a model spring. Consequently, this change in stiffness will affect the overall dynamic response of the structure under an external load. This formulation was also presented in our recently published papers [42-43]. A cantilever beam is selected and the crack is modeled as a massless torsional spring as shown in Figure 4. The stiffness of torsional spring k_t is

given by Ostachowicz et al. [6] as shown in Eq. (1). The relationship between the crack depth and dynamic response in terms of natural frequency is obtained using the Rayleigh quotient.

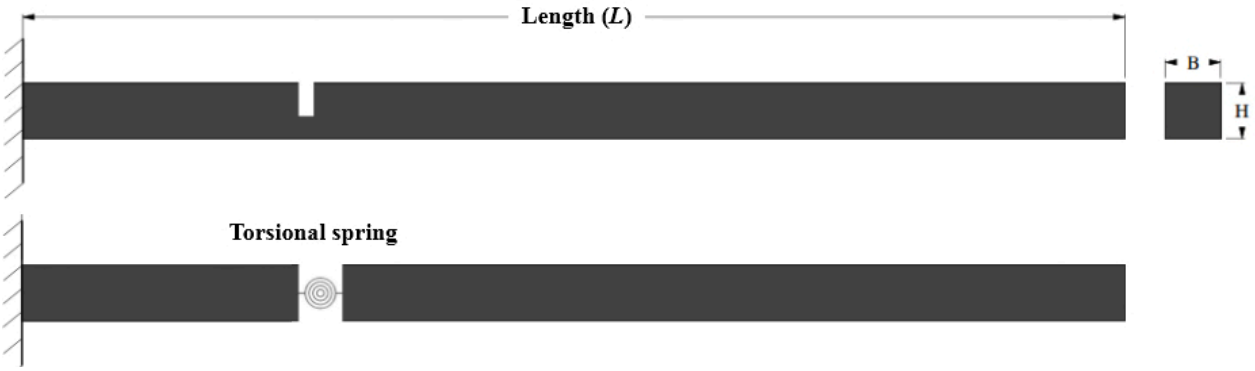

Figure 4: Cantilever beam with crack analyzed as mass less torsional spring.

$$k_t = \frac{E\,B\,H^2}{72\,\pi\,F\left(\frac{t_c}{H}\right)} \tag{1}$$

$$F\left(\frac{t_c}{H}\right) = 0.638\left(\frac{t_c}{H}\right)^2 - 1.035\left(\frac{t_c}{H}\right)^3 + 3.720\left(\frac{t_c}{H}\right)^4 - 5.177\left(\frac{t_c}{H}\right)^5 + 7.553\left(\frac{t_c}{H}\right)^6 - 7.332\left(\frac{t_c}{H}\right)^7 + 2.491\left(\frac{t_c}{H}\right)^8 \tag{2}$$

where, B is width of the beam, H is height of the beam, t_c is crack depth, E is modulus of elasticity and $F\left(\frac{t_c}{H}\right)$ is crack function. Free bending vibration of a beam is identified by a well-known differential equation as shown in Eq. (3). Applying boundary conditions $y(0) = 0,\ y'|_{@x=0} = 0$ and $y''|_{@x=L} = 0$ to find mode shape as shown in Eq. (4) - Eq. (6).

$$EI\frac{\partial^4 y}{\partial x^4} + \rho A\frac{\partial^2 y}{\partial t^2} = 0 \tag{3}$$

$$y(x) = y_0\left[1 - \cos\left(\frac{\pi x}{2L}\right)\right] \tag{4}$$

$$y' = y_0\left(\frac{\pi}{2L}\right)\left[\sin\left(\frac{\pi x}{2L}\right)\right] \tag{5}$$

$$y'' = y_0\left(\frac{\pi}{2L}\right)^2\left[\cos\left(\frac{\pi x}{2L}\right)\right] \tag{6}$$

where x is the crack location from fixed end and y_0 is assumed mode shape deflection. The bending moment can be derived from beam curvature and flexural rigidity (EI) as shown in Eq. (7). The total strain energy can be derived from direct strain and strain energy due to bending as shown in Eq. (8) - Eq. (9). The change in natural frequency and strain energy can be found out using Eq. (10) - Eq. (12), presented by Majid et. Al [44]. They calculated the natural frequency and the corresponding mode shape of cracked beam using the Generalized Differential Quadrature (GDQ) method.

$$M = EIy'' \tag{7}$$

$$u = \frac{EI}{2}\int_0^L (y'')^2\,dx \tag{8}$$

$$u = \frac{EI}{64}\pi^4\left[\frac{1}{L^3}\right](y_o)^2 \tag{9}$$

$$\Delta u = \frac{M^2}{2k_t} \tag{10}$$

$$\Delta\omega_{nc} = \frac{\Delta u}{2u}\omega_n \tag{11}$$

$$\omega_{nc} = \omega_n - \Delta\omega_{nc} \tag{12}$$

where M is bending moment, u is strain energy, Δu is change in strain energy, ω_{nc} is natural frequency of a cracked beam and $\Delta\omega_{nc}$ is difference between the natural frequencies of the uncracked and cracked beam. Eq. (3) - Eq. (12). can be merged to formulate a generalized equation for ω_{nc} as shown in Eq. (13). This equation summarizes all the variables used in the analytical formulation. It can be inferred that the natural frequency of cracked beam is independent of initially assumed value of mode shape and material properties. However, it depends on the natural frequency of the uncracked beam (or at the previous crack depth), crack location and geometrical parameters of the specimen. An accelerometer is mounted at the end of the specimen to measure the dynamic response at different crack depths as shown in Figure 5. Therefore, the undamped natural frequency of the beam with end mass is given by Irvin [45] as shown in Eq. (14).

$$\omega_{nc} = \left[1 - \left\{\frac{72\,\pi\, I\, F\left(\frac{t_c}{H}\right)}{BH^2L}\left(\cos\left\langle\frac{\pi x}{2L}\right\rangle\right)^2\right\}\right]\omega_n \tag{13}$$

Figure 5: Schematic of cantilever beam with end mass

$$\omega_{nm} = \sqrt{\frac{3EI}{(0.2235\rho_L L + m)L^3}} \tag{14}$$

where, ω_{nm} is the natural frequency of beam with end mass, ρ_L is the mass per unit length and m is the end mass (mass of accelerometer).

$$\omega_{nc} = \left[1 - \left\{\frac{72\pi\, I\, F\left(\frac{t_c}{H}\right)}{BH^2L}\left(\cos\left\langle\frac{\pi x}{2L}\right\rangle\right)^2\right\}\right]\sqrt{\frac{3EI}{(0.2235\rho L + m)L^3}} \tag{15}$$

Eq. (13) - Eq. (14) can be used to get Eq. (15), where E is the temperature depended modulus of elasticity of the beam. The variation in E can be used to find the cracked beam natural frequency under different temperatures. This modal frequency can be used to determine the crack depth using dynamic response under thermo-mechanical loads. The value of the change in stiffness parameter with temperature variation from none-heating to 200°C is shown in Table 1 [46].

Table 1: Values of modulus of elasticity (E) with temperature [46]

Temperature [°C]	Modulus of elasticity [Gpa]
Non-heating	73.0
50	72.7
100	70.4
150	68.6
200	66.3

4.2 Numerical simulation under thermo-mechanical loads

Dynamic response is estimated for both initially seeded and propagating crack using numerical simulations. In establishing a numerical relationship between fundamental frequency/amplitude and crack depth, the finite element modal analysis is carried out on the modeled specimens using ANSYS©v14.0 as shown in Figure 6. The modal and harmonic modules of

ANSYS© workbench are used to obtain the natural frequency and amplitude of the specimen at a crack depth ranging from 0.5 mm to 2.5 mm with increments of 0.5 mm as shown in the inset of Figure 6. The geometry of the crack surface is considered as a rectangle with a constant width of 0.2 mm.

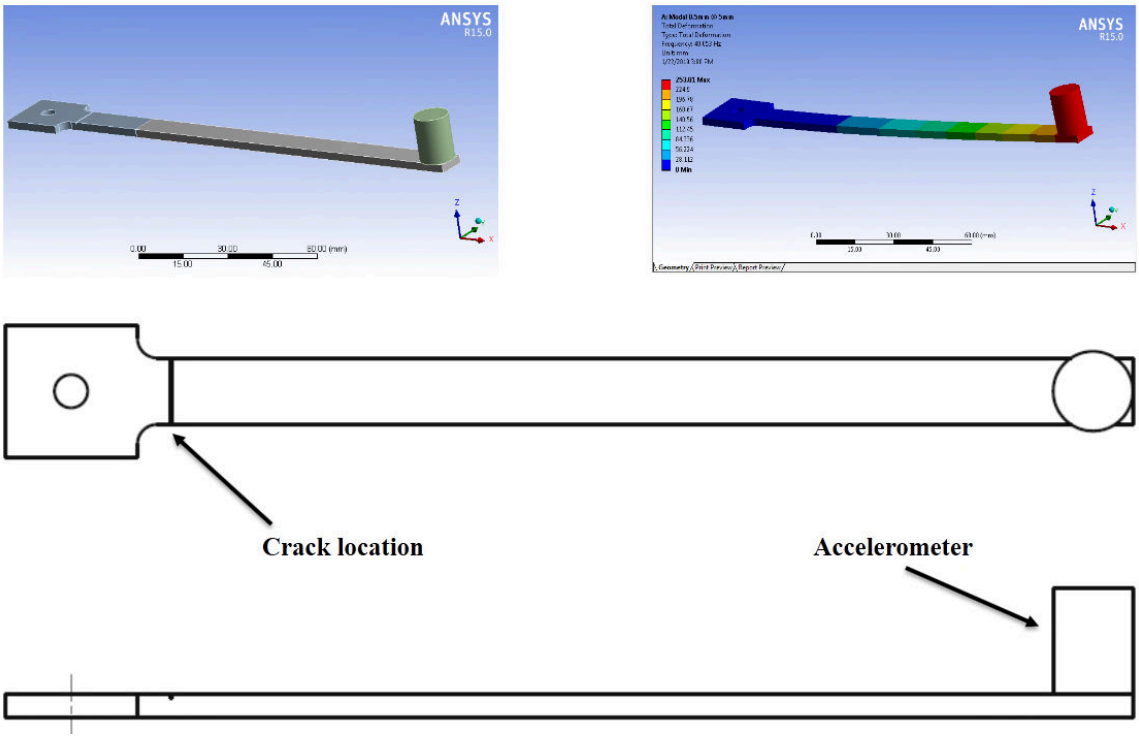

Figure 6: ANSYS© model showing predefined crack and accelerometer with simulation results

5 Results and discussion

5.1 Initially seeded crack with different crack depths

Four configurations (Uncracked, crack at 5% of L, crack at 10% of L and crack at 15% of L) are selected. A pre-defined crack is induced with depth ranges from 0.5 mm to 2.5 mm with an increment of 0.5 mm. In the start of each experiment, a fresh specimen with pre-defined crack depth is mounted on the test rig and the accelerometer is installed at the free end. The setup is capable of analyzing and recording the in-situ dynamic response of the specimen while vibrating at any frequency. An impact test is carried out to determine the fundamental frequency of a fresh specimen experimentally. The specimen is set to run at an operating frequency using the signal generator. Initially, this operating frequency is equal to the fundamental frequency obtained from the impact test. Simultaneously, the amplitude response of the acceleration is also monitored. The results of the experiments are compiled and plotted for each of the specimens with a predefined crack depth ratio at a selected temperature. The analytical, numerical and experimental results are plotted at a different temperature as shown in Figure 7. This figure is presented to establish the credibility of the experimental results. The results are found in good agreement with numerical and analytical calculations. The difference in results is within 10% error at all temperatures. Lower experimental values are observed compared to analytical/numerical approaches, which may be due to higher stiffness value taken for analytical and numerical simulation results.

Natural frequency and amplitude are plotted in Figure 8 & Figure 9 for crack located at 5%, 10% and 15% of total length for temperature varies from non-heating to 200ºC. The natural frequency is higher for crack located at 15% of total length for all temperature value, showing that the stiffness is less sensitive for crack located away from the fixed support. Crack located near fixed support makes the structure more elastic, thus, they have a lower value of structural damping. Subsequently, the structure having lower natural frequency has the higher value of amplitude response under same loading. It shows that the material damping is not affected by crack location. However, structural damping can change with crack location. This can also be validated with the response of the underdamped system that the reduction in damping and natural frequency will result in higher amplitude as shown in Eq. (16) [47].

$$x = X\, e^{-\xi \omega_n \tau} \tag{16}$$

where, x is the instantaneous amplitude, ξ is the damping and τ is the time.

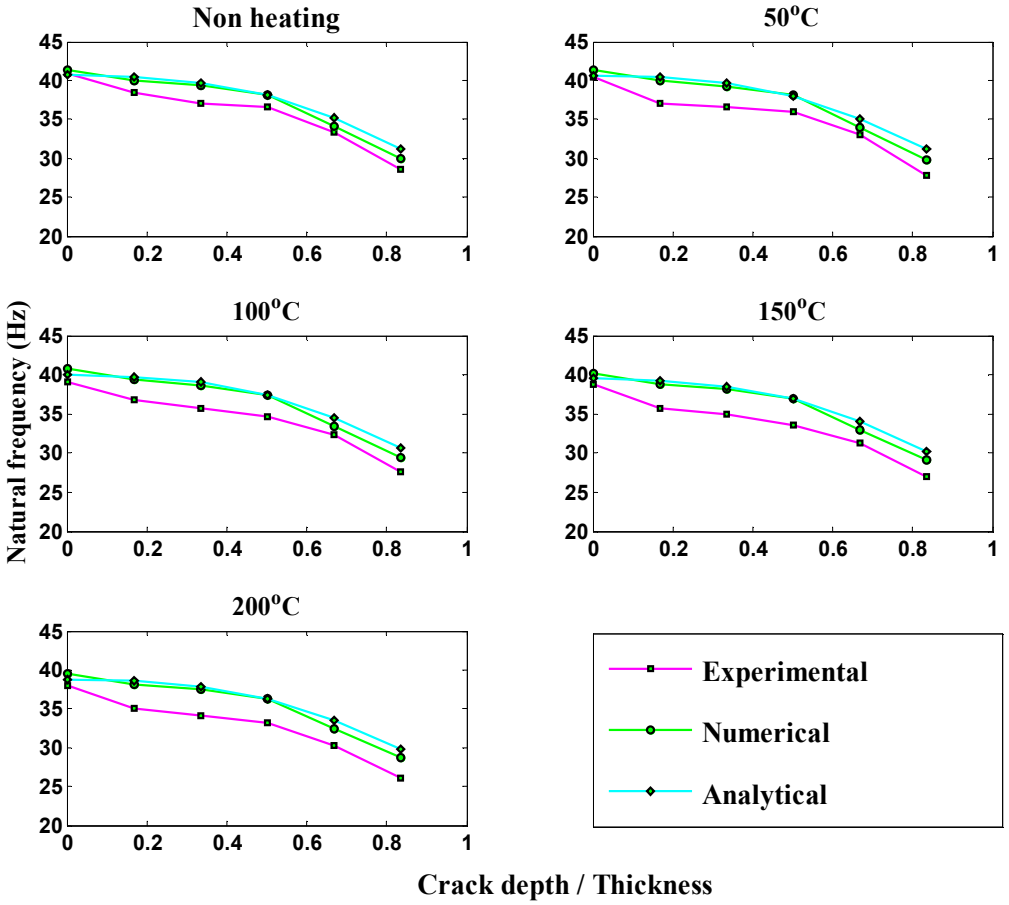

Figure 7: Natural frequency VS crack depth ratio for initially seeded crack located at 5% of total length

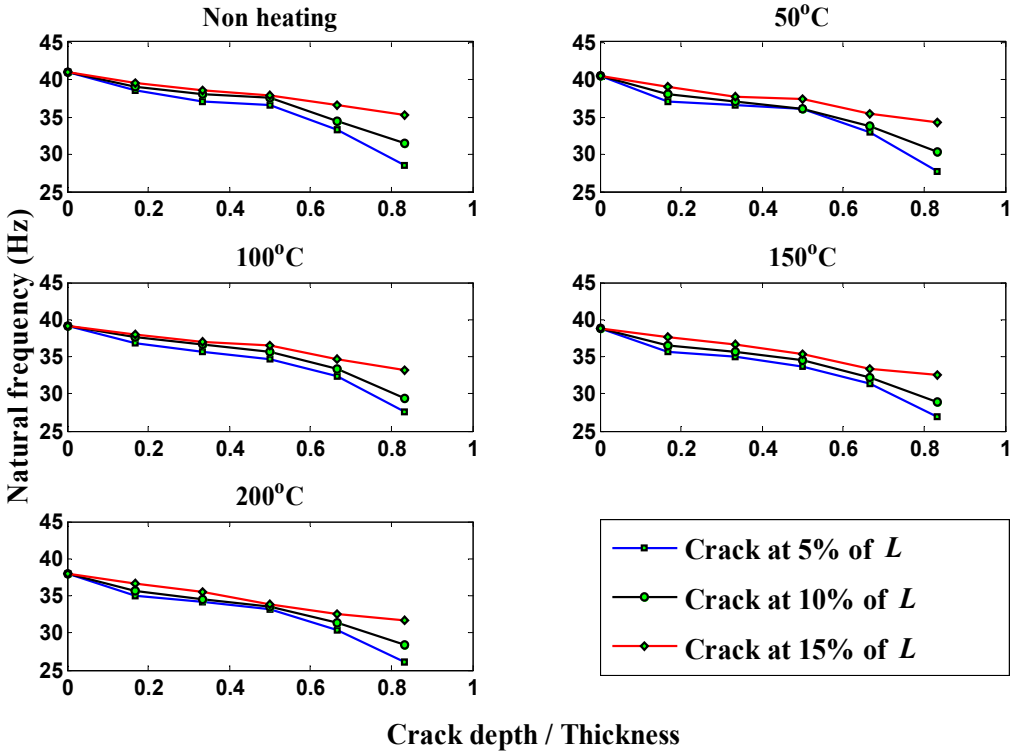

Figure 8: Experimental natural frequency VS crack depth ratio for initially seeded crack located at different positions.

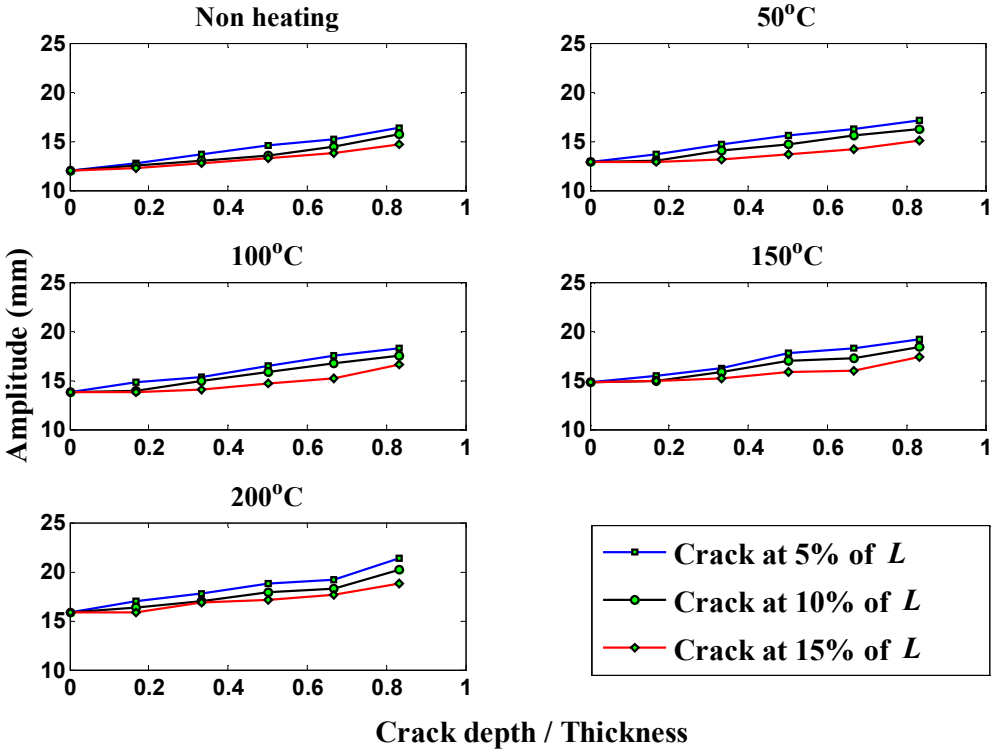

Figure 9: Experimental amplitude VS crack depth ratio for initially seeded crack located at different positions.

In order to perceive the effect of temperature variation, the frequency and amplitude response of initially seeded crack is plotted for temperature varying from non-heating to 200°C as shown in Figure 10. The natural frequency of the structure is reduced with increased temperature for the same amount of damage. Conversely, amplitude increases due to a reduction in structural damping. This shows that the temperature can increase the failure rate under thermo-mechanical loads.

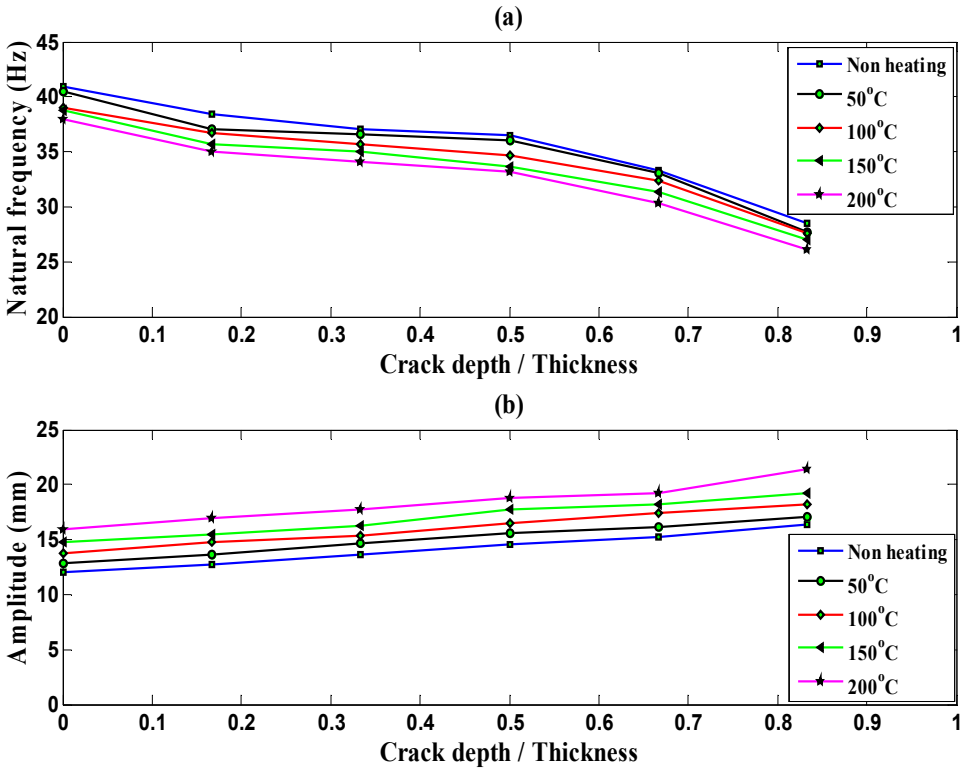

Figure 10: Experimental natural frequency & amplitude for initially seeded crack at different temperatures located at 5% of total length.

5.2 Propagating crack

In the start of each experiment, a fresh specimen of crack depth 0.5 mm is mounted on a shaker at different temperatures. The specimen is set to run on its natural frequency and amplitude is measured. The amplitude drop is used as a sign of change in the natural frequency of the specimen. The impact test is carried out again with a light wooden mallet to find out the new modal frequency. This procedure is repeated until the catastrophic failure of the specimen. At the same instance, an image is captured using a microscope to measure crack depth as shown in Figure 11. Natural frequencies and its respective drops with respect to crack depth ratio are plotted as shown in Figure 12.

The value of natural frequency at 0.5 mm crack depth is the fundamental frequency of the specimen. This crack will start propagating once the load is applied and the specimen is forced to vibrate on its natural frequency. This propagation will reduce the stiffness ultimately causing a decrease in the natural frequency as depicted by the curves. The lowest value is achieved until its catastrophic failure. Additionally, the difference of amplitude response for propagating crack is measured with reference to initial crack depth as shown in Figure 13 for crack located at 5% of total length at defined temperature range. Due to a decrease in stiffness with propagating crack the response will increase against the same amount of loading.

The results for natural frequency and amplitude are similar to initially seeded crack in terms of trend. Crack located at 15% of total length has the highest value of natural frequency and lowest amplitude at the same amount of damage. An important phenomenon is observed during crack propagation, that the natural frequency did not show any significant variation against subsurface cracking at a crack depth near 0.5 mm. Therefore, it was very difficult to predict the closest point when subsurface cracking has started. The microscope does not show any change in the initially seeded crack as shown in Figure 12. Conversely, a sharp drop in the amplitude at 0.5 mm shows that the subsurface crack propagation has started which can help in preventive maintenance as shown in Figure 13. Therefore, the amplitude response can be given extra importance under thermo-mechanical loads which can increase the crack propagation rate by reducing the structural stiffness.

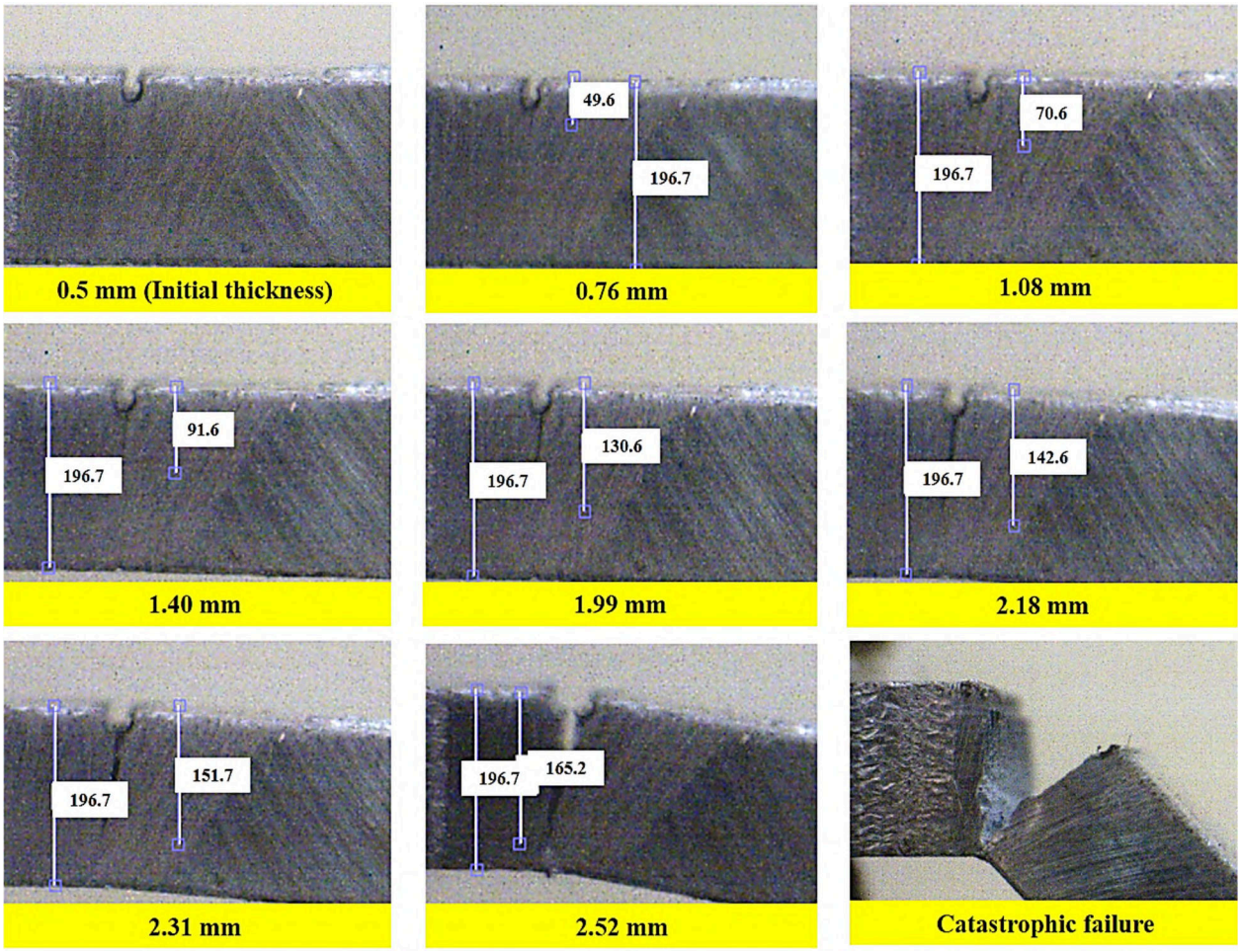

Figure 11: The specimen showing the evolution of crack propagation.

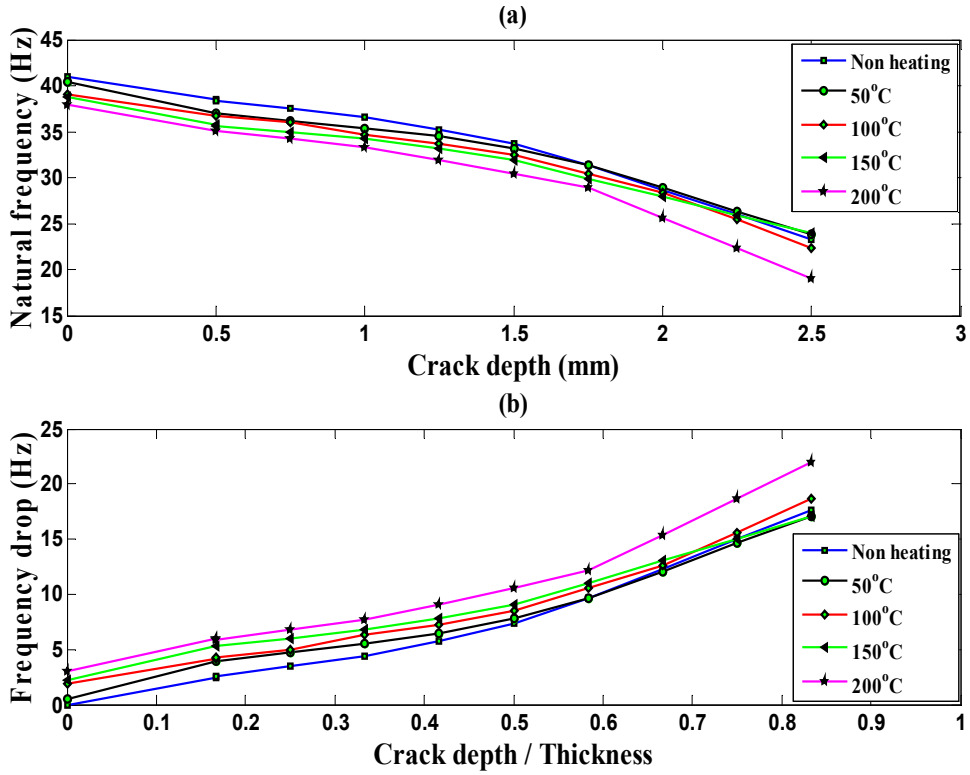

Figure 12: (a)Natural frequency VS crack depth for propagating crack located at 5% of total length, (b)Natural frequency drop VS crack depth ratio for propagating crack located at 5% of total length

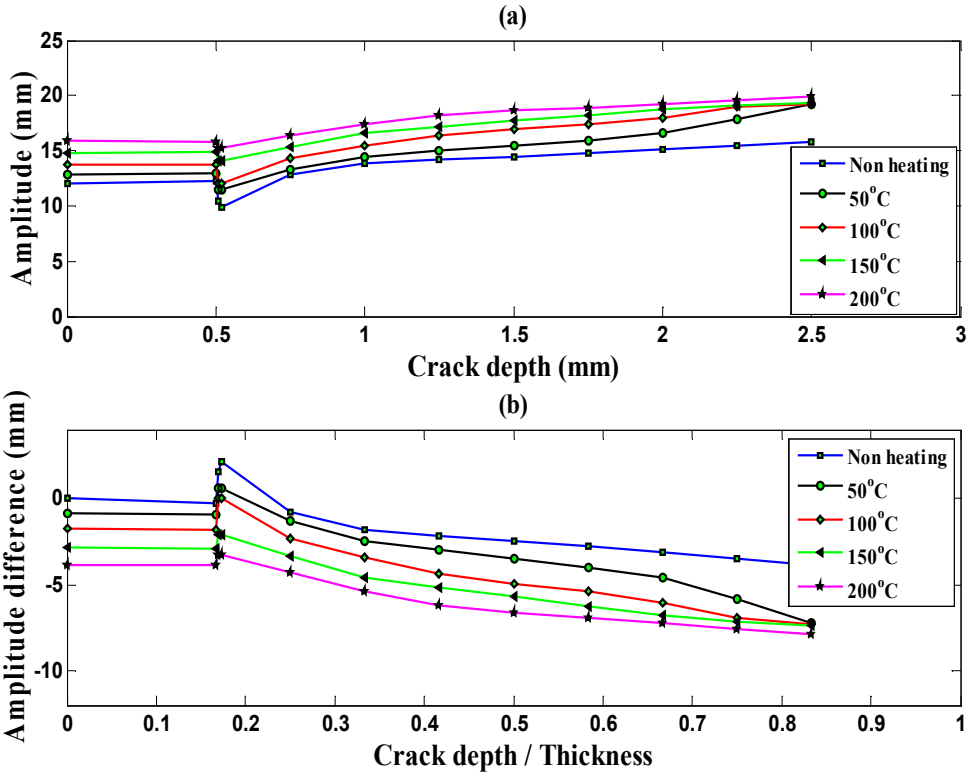

Figure 13: (a)Amplitude VS crack depth for propagating crack located at 5% of total length, (b) Amplitude difference VS crack depth ratio for propagating crack located at 5% of total length

5.3 Empirical correlations

The proposed methodology can identify both crack depth and location which consists of an empirical relationship between the crack depth, crack location, temperature, natural frequency and amplitude of the selected beam. A significant number of

experiments are required to form an empirical relation. This empirical relation is expected to predict the crack depth using natural frequency drop, amplitude difference, and temperature. A criterion known as percentage replication (PR) is commonly used to define the percentage of reliability of the results based on experimental data as shown in Eq. (17) [48].

$$\mathrm{PR} = \quad 100 \left[1 - \frac{L_p}{n}\right] \tag{17}$$

where, L_p is the number of varying parameters and n is the total number of experiments. In this work total three locations and five temperatures are considered. For each set of location and temperature, three specimens are tested. This will make the reliability of data set of 82%, and suggest that the predicted results based on these empirical correlations will have an accuracy of 82%.

In the proposed methodology, the response and temperature are taken as input. Using the available data, interpolation is performed to find out three combinations of crack depth and location for frequency drop and amplitude difference separately. These three combinations are pragmatic because of the fact that the same frequency drop and amplitude difference can be achieved at three different combinations of crack location and depth. Later the difference of each set of crack depth at specific location obtained by frequency drop and amplitude difference is taken. The minimum difference in predicted values based on frequency drop and amplitude difference will suggest the most accurate crack depth and location. A detailed schematic of predicting crack depth and location is shown in Figure 14.

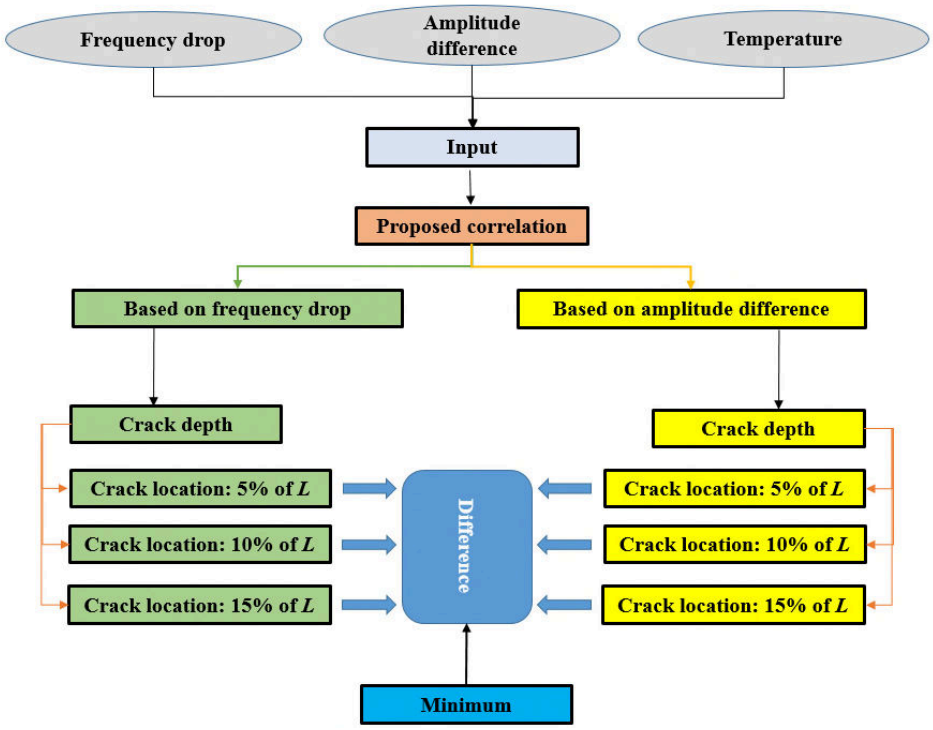

Figure 14: Schematic for predicting crack depth and location

There will be six global correlations for three locations based on specific response parameter. From these correlations six crack depths are evaluated from six global correlations, three by using the natural frequency difference and three by amplitude difference. One set of value of crack depth represents one location. Therefore, the difference of these crack depths belongs to one location which will help in deciding the final crack location. The position where the crack depth difference is minimum is the actual physical location of crack. These empirical correlations can be used to get the crack propagation from initiation to failure. The visually measured crack depth values are compared with the values obtained from Eq. (15) and are found in good agreement.

A polynomial curve fitting is performed on available data to obtain a global empirical equation which can accommodate a range of frequency and length of the specimen as shown in Eq. (18-20). Eq. (19) and Eq. (20) are formulated based on frequency drop, amplitude difference and temperature. Therefore, first matrix is for polynomial coefficient and the other is based on corresponding value of dynamic response parameters and temperature. Crack depth is plotted as a function of frequency drop, amplitude difference, and temperature as shown in Figure 15 & Figure 16. This polynomial curve fit can accommodate most of the available data point. However, few of are still not covered the prediction percentage will be higher in the vicinity of these points.

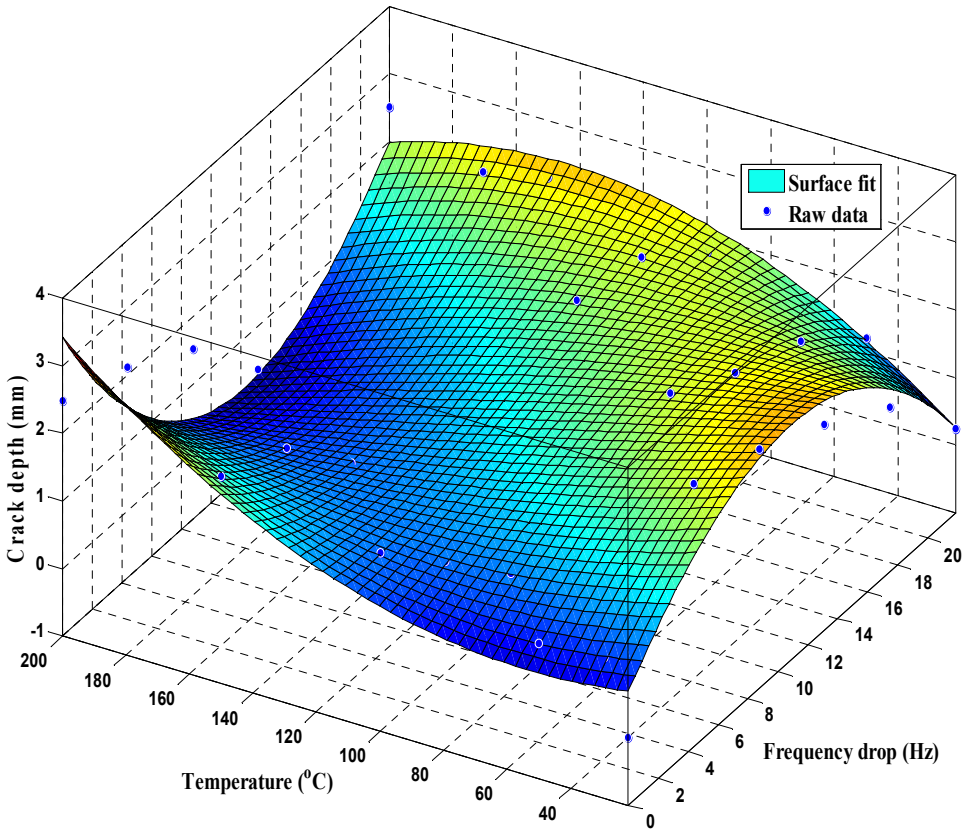

359
360 Figure 15: Experimental and surface fit data for empirical correlation based on frequency drop for crack located at 5% of *L*

361

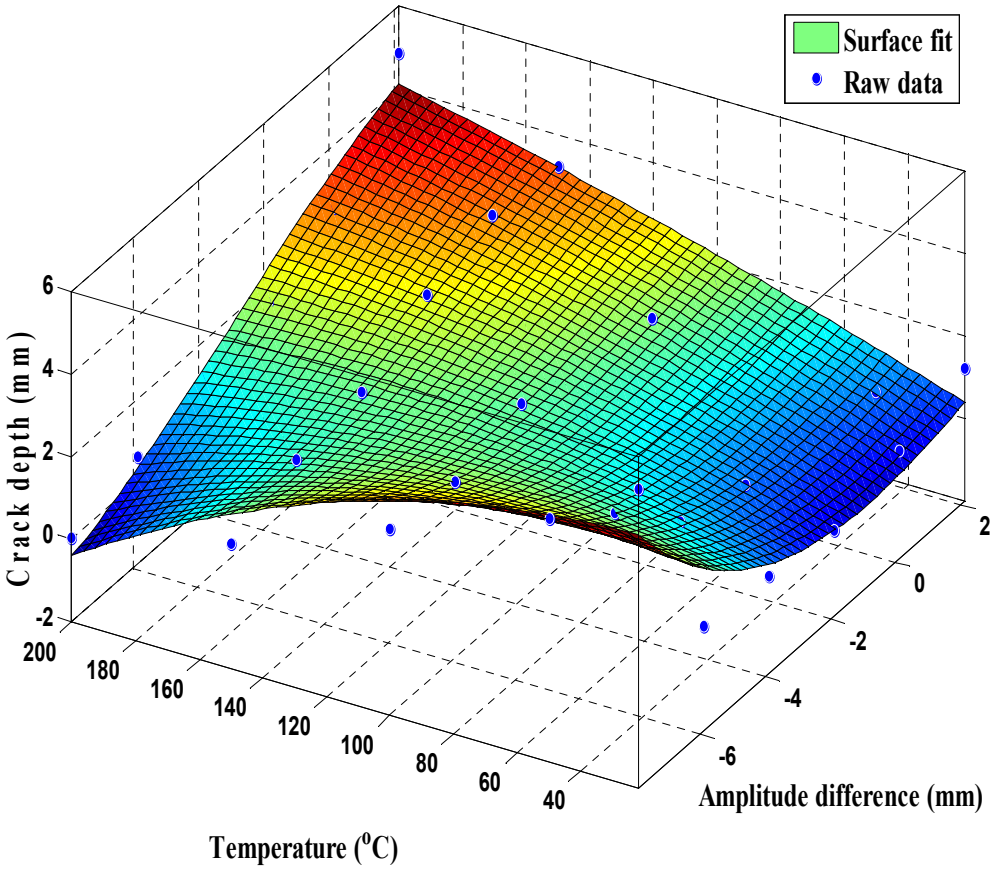

362
363 Figure 16: Experimental & surface fit data for empirical correlation based on amplitude difference for crack located at 5% of *L*

Experimental results are plotted with the results obtained via a global empirical equation, and found in good agreement. The global empirical relation can be used to predict around 82% of available date for validation within 10% of error. The presence of a crack can change the material properties of the specimen which ultimately cause the drop in its natural frequency and amplitude variation till catastrophic failure. Mathematically, empirical correlations can be obtained from these trends which can be used to estimate the crack depth and location, if the frequency drop/amplitude difference and temperature are known. This equation can be a very useful for in-situ damage assessment of metallic structures. These empirical correlations can be used as a very effective damage assessment tool in in-situ condition. The accuracy of damage prediction is excellent at higher frequency drop and amplitude difference.

$$t_c = f(\Delta\omega_{nc}, \Delta D, T) \tag{18}$$

$$t_{cf} = A_f + B_f\Delta\omega_{nc} + C_f T + D_f{\Delta\omega_{nc}}^2 + E_f\Delta\omega_{nc} T + F_f T^2 + G_f{\Delta\omega_{nc}}^3 + H_f{\Delta\omega_{nc}}^2 T + I_f\Delta\omega_{nc} T^2 \tag{19}$$

$$t_{cD} = A_D + B_D\Delta D + C_D T + D_D\Delta D^2 + E_D\Delta D T + F_D T^2 + G_D\Delta D^3 + H_D\Delta D^2 T + I_D\Delta D T^2 \tag{20}$$

where, t_{cf} is crack depth prediction based on natural frequency drop, t_{cD} is crack depth prediction based on amplitude difference, $\Delta\omega_{nc}$ is natural frequency drop, ΔD is amplitude difference, T is selected temperature, $A_f, B_f, C_f, D_f, E_f, G_f, H_f, I_f$ are the coefficients of empirical correlation derived using frequency drop and temperature data for crack located at 5% of L, $A_D, B_D, C_D, D_D, E_D, G_D, H_D, I_D$ are the coefficients of empirical correlation as shown in Table 2.

Table 2: Coefficients of empirical correlations Eq. (18)

Coefficients	**Crack location**		
	5 % of *L*	**10 % of *L***	**15 % of *L***
A_f	0.9367	0.8726	0.8574
B_f	0.359	0.3701	0.3973
C_f	-0.01433	-0.01106	-0.008917
D_f	-0.01637	-0.01828	-0.02223
E_f	-0.001936	-0.002136	-0.002331
F_f	0.0001338	0.00012	0.0001143
G_f	-0.000147	-5.192e-005	0.0001004
H_f	0.0002067	0.0002018	0.0002062
I_f	-1.286e-005	-1.165e-005	-1.146e-005
A_D	0.5348	-0.1923	-0.5979
B_D	0.6342	0.3507	0.1834
C_D	0.003625	0.02056	0.02765
D_D	0.08744	0.0629	0.09089
E_D	-0.01193	-0.00784	-0.0004958
F_D	1.201e-005	-4.185e-005	-5.088e-005
G_D	-0.01013	-0.008389	-0.002902
H_D	-0.001533	-0.00109	-0.000517
I_D	2.413e-005	2.233e-005	1.016e-005

6 Validation of empirical correlations

6.1 Validation based on available data

Initially proposed empirical correlations are validated with the same experimental values which are used to develop these correlations using dynamic response and temperature values. These values are given as input to Eq. (19) and crack depth based on frequency and amplitude are calculated at known crack locations. Experimental results are plotted with the results obtained via a global empirical equation, and found in good agreement as shown in Figure 17 to Figure 22.. Mathematically, empirical correlations can be obtained from these trends which can be used to estimate the crack depth and location, if the frequency drop/amplitude difference and temperature are known.

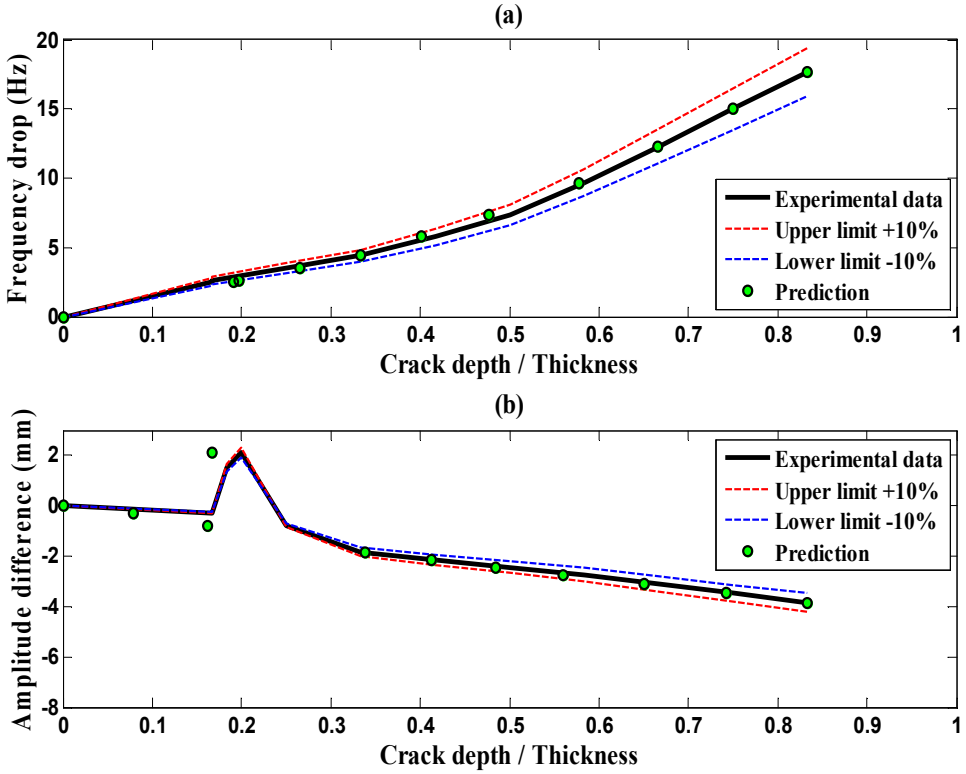

Figure 17: (a) Comparison of experimental and prediction results based on frequency drop (b) Comparison of experimental and prediction results based on amplitude difference for crack located at 5% of *L* at non-heating condition

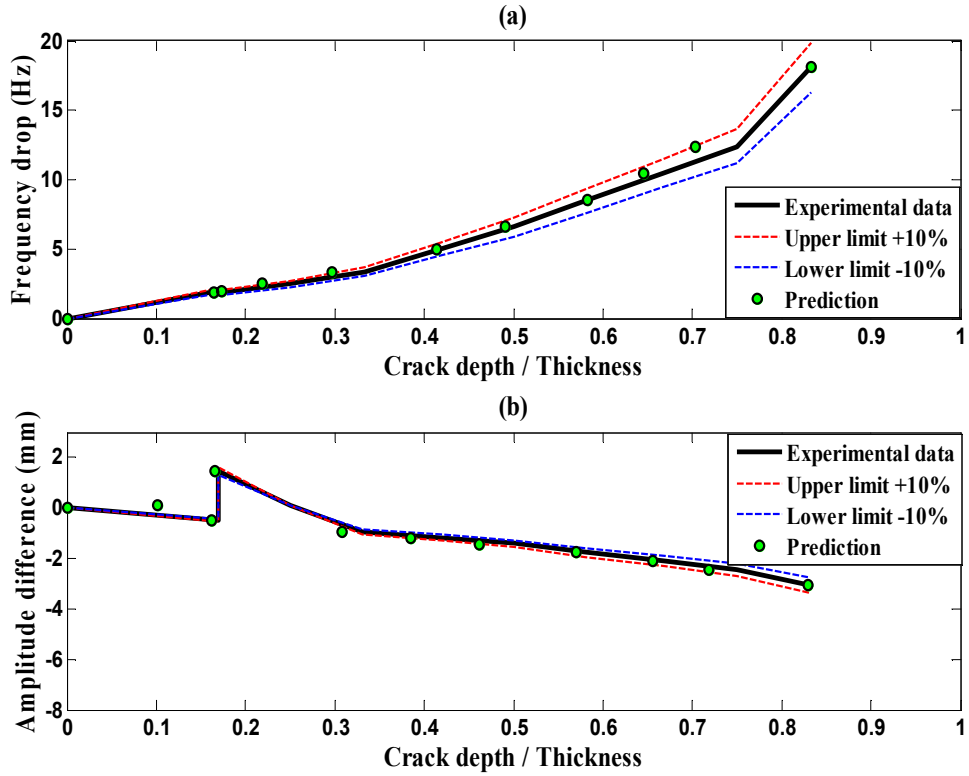

Figure 18: (a) Comparison of experimental and prediction results based on frequency drop (b) Comparison of experimental and prediction results based on amplitude difference for crack located at 10% of *L* at non-heating condition

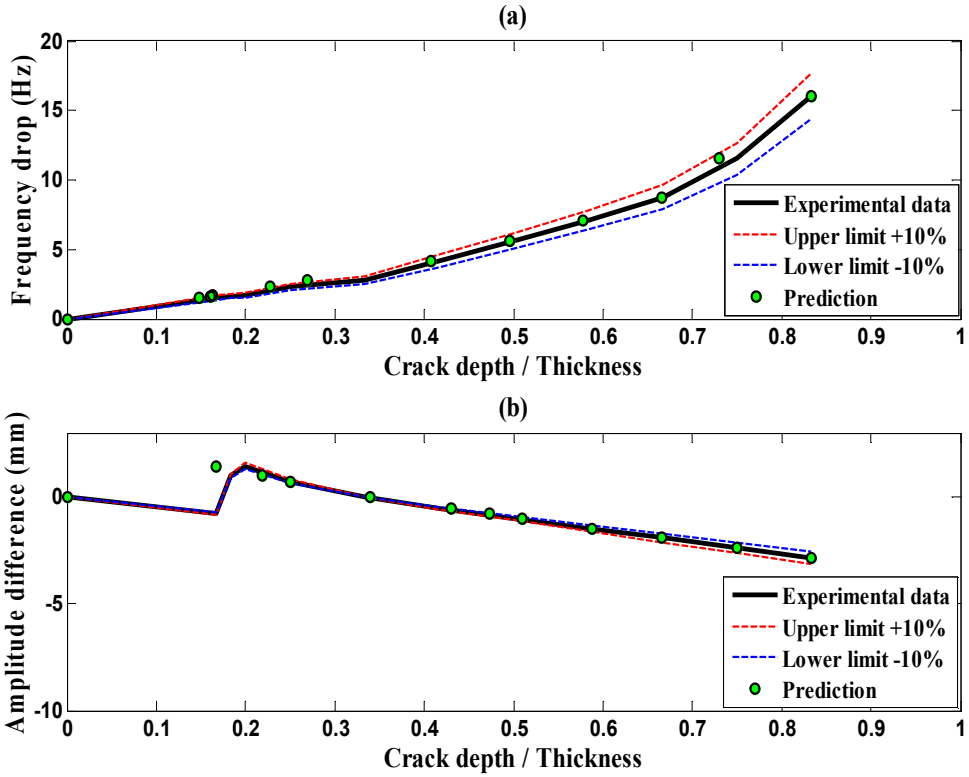

Figure 19: (a) Comparison of experimental and prediction results based on frequency drop (b) Comparison of experimental and prediction results based on amplitude difference for crack located at 15% of *L* at non-heating condition

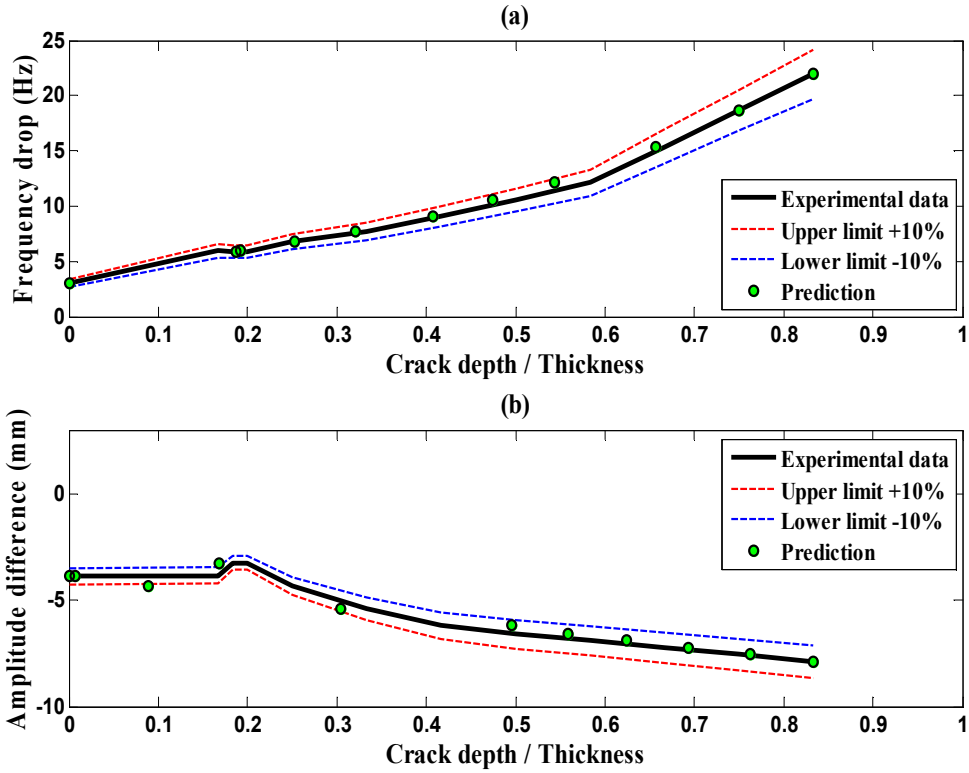

Figure 20: (a) Comparison of experimental and prediction results based on frequency drop (b) Comparison of experimental and prediction results based on amplitude difference for crack located at 5% of *L* at 200°C

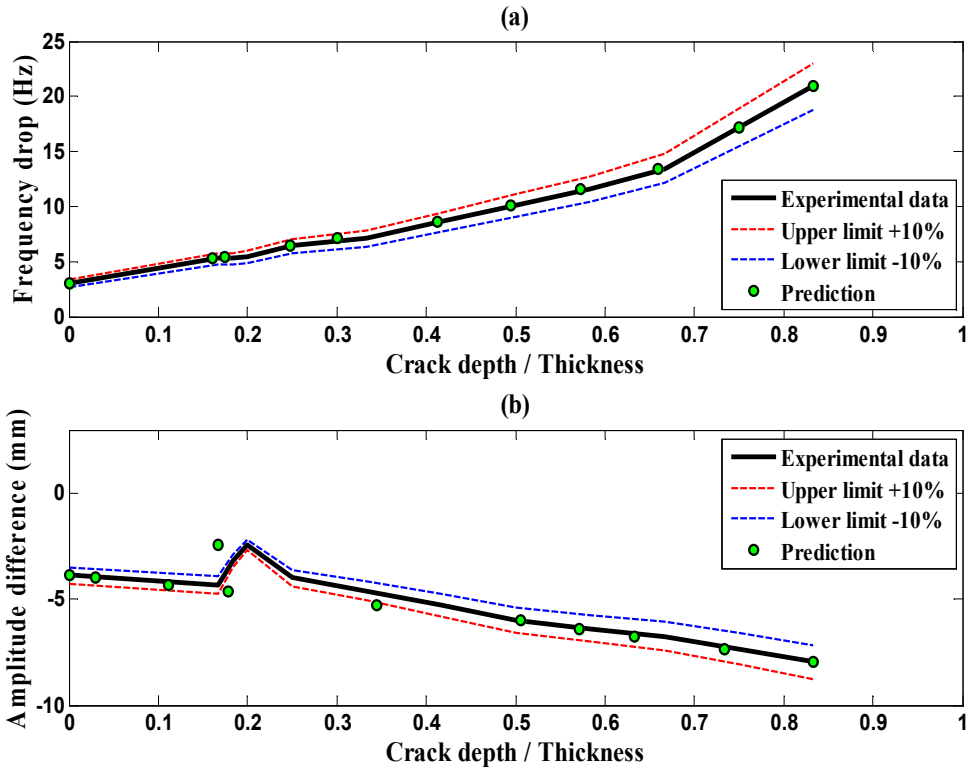

Figure 21: (a) Comparison of experimental and prediction results based on frequency drop (b) Comparison of experimental and prediction results based on amplitude difference for crack located at 10% of *L* at 200°C

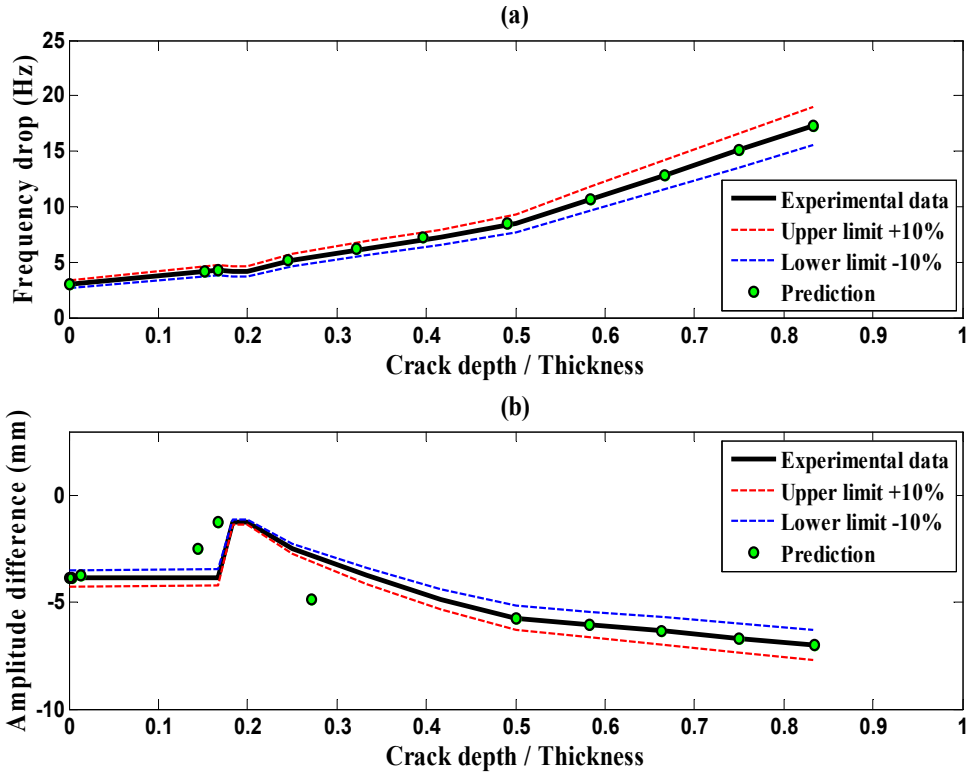

Figure 22: (a) Comparison of experimental and prediction results based on frequency drop (b) Comparison of experimental and prediction results based on amplitude difference for crack located at 15% of L at 200°C

Consistent results are obtained at all the temperature loads. Therefore, two extreme conditions are presented including non-heating and 200°C. The results show that the proposed tool is very useful for accurate damage assessment. The accuracy of the prediction is continuously improving with the increase in frequency drop and amplitude difference. This tool can be used with either of the response parameters and also valid near sub-surface cracking using amplitude difference. The basic limitation of prediction based on frequency drop is that the same reduction can be achieved with a different combination of crack depth and location. Therefore, the amplitude difference can be used in conjunction with a frequency drop to overcome this limitation. This tool is validated with ±10% prescribed range of crack depth prediction.

6.2 Validation for arbitrary data

For general validation of empirical correlations, total nine samples are used for damage assessment at arbitrary input parameters. Out of nine, three for each location are considered for different response values and temperatures. The respective frequency drop and amplitude difference are measured as shown in Table 3. The prediction results using the proposed correlation are found very close to actual as shown in Table 4. Images for experimental validation are shown in Figure 23. The crack depth to thickness ration can be calculated as shown in Eq. (21).

$$t_c/t = \mathrm{F1/F2} \tag{21}$$

where,t_c is crack depth, t is specimen thickness, F1 is the crack measurement value on image and F2 is the thickness measurement value on image using *MATLAB imtool.*

Table 3: Measured response of nine samples for validation

Crack location (% of L)	Temp. [C°]	Freq drop [Hz]	Amplitude difference [mm]
5	75	8.44	-2.10
5	110	10.24	-1.88
5	125	8.41	-3.88
10	175	9.11	-5.53
10	190	16.21	-6.84
10	90	5.20	-2.96
15	60	7.59	-5.44
15	135	8.48	-6.01
15	165	11.88	-6.22

Table 4: Prediction using proposed empirical correlation

Temp. [C°]	Crack depth / Thickness					Crack location (% of L)	
	Actual t_c/t	Prediction t_{cf}/t	% Error	Prediction t_{cD}/t	% Error	Actual	Prediction
75	0.469	0.499	6.40	0.464	1.07	5	5
110	0.544	0.561	3.13	0.519	4.60	5	5
125	0.507	0.464	8.48	0.479	5.52	5	5
175	0.516	0.487	5.62	0.532	3.10	10	10
190	0.754	0.736	2.39	0.783	3.85	10	10
90	0.314	0.325	3.50	0.337	7.32	10	10
60	0.557	0.545	2.15	0.581	4.31	15	15
135	0.574	0.533	7.14	0.59	2.79	15	15
165	0.606	0.665	9.74	0.559	7.76	15	15

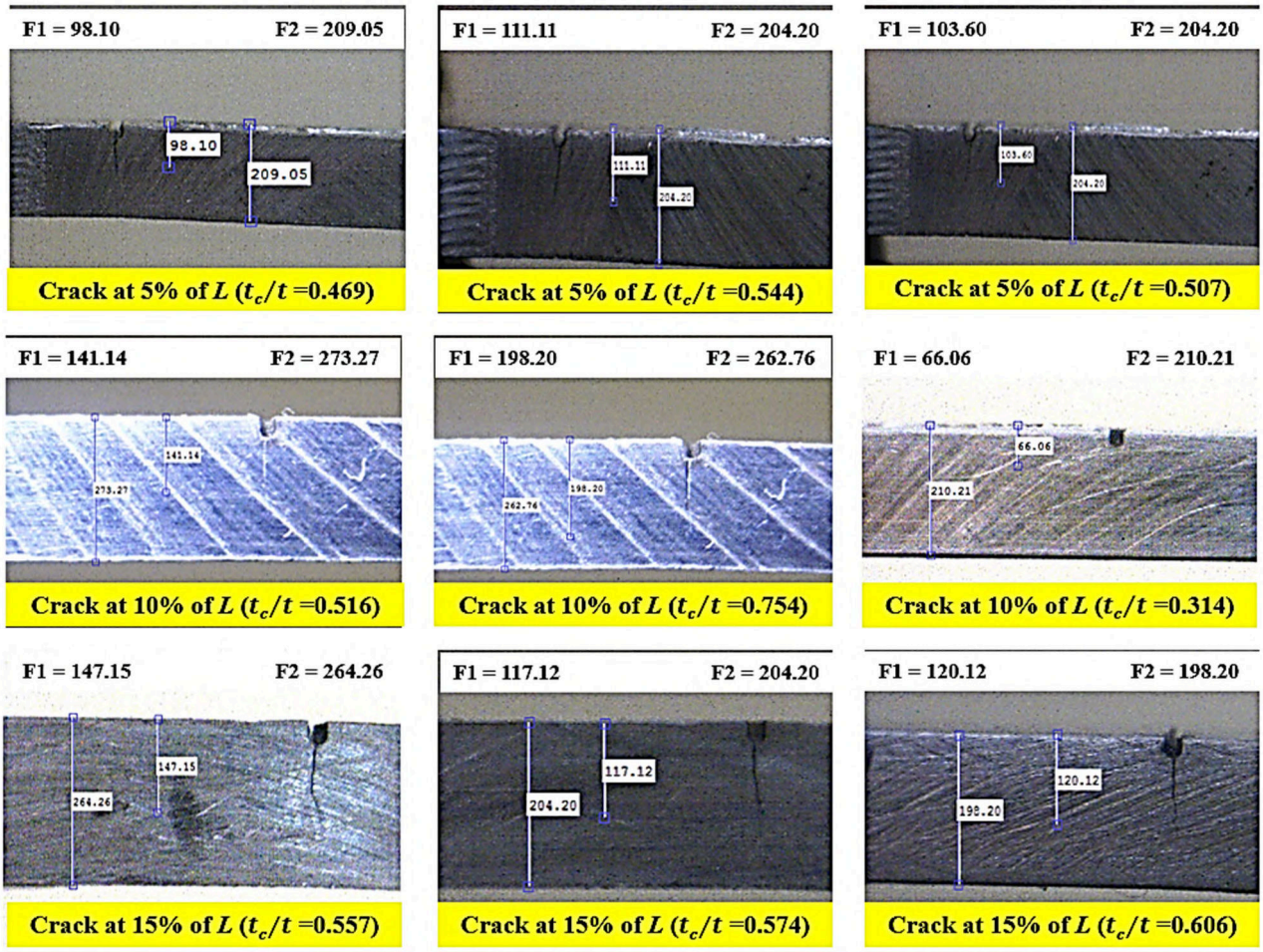

Figure 23: Images of specimens for experimental validation

7 Conclusion

A methodology is proposed to predict the crack depth in an Aluminum 2024 cantilever beam, operating at a modal frequency by its dynamic response values including frequency drop and amplitude difference due to stiffness variation. The methodology is based on in-situ operating condition to predict the depth of a propagating crack under thermo-mechanical loads. Experimental data for increasing crack depth at different locations and temperatures is gathered. Based on the comprehensive results, a trend is obtained to establish relationships among crack depth, location and temperature for the first time for a cantilever beam operating under thermo-mechanical loads. Higher temperature reduces stiffness consequently frequency is also reduced. This will cause to vibrate the specimen at higher amplitude under same loading. The similar phenomenon is observed for crack located away from the fixed support. Distinguish results are obtained for amplitude response in which the subsurface cracking is evident without showing any increase in crack propagating. A detailed

schematic is established to predict crack location and depth. Empirical relations based on global curve fit are presented using dynamic response and temperature to formulate a robust tool. This tool is validated with available as well as arbitrary data. The predicted results are well within 10% of prediction range using frequency drop for all configurations. Further, this procedure can also be used to analyze the crack propagation path and its rates without dismantling the structural element from its routine operations.

References

1. S.W. Doebling, C.R. Farrar, M.B. Prime, A summary review of vibration-based damage identification methods, Shock and vibration. 30 (1998) 91-105.
2. W. Fan, P. Qiao, Vibration-based damage identification methods a review and comparative study, Structure health monitoring. 10 (2011) 83-111.
3. S. Das, P. Saha, S.K Patro, Vibration-based damage detection techniques used for health monitoring of structures a review, J. of civil structure health monitoring. 6 (2016) 477–507.
4. M.K. Khorshidi, D. Soltani, Diagnosis of type, location and size of cracks by using generalized differential quadrature and Rayleigh quotient methods, J. of theoretical and applied mechanics. 43(2013) 61–70.
5. J.A. Loya, L. Rubio, J. Fernandez-Saez, Natural frequencies for bending vibrations of Timoshenko cracked beams, Continuum mechanics and structural analysis. 290 (2006) 1-14.
6. W.M. Ostachowicz, M. Krawczuk, Analysis of the effect of cracks on the natural frequencies of a cantilever beam, J. of Sound & vibration. 150 (1991) 191-201.
7. A.C. Batihan, Vibration analysis of cracked beams on elastic foundation using Timoshenko beam theory. MS thesis, Middle East Technical University. 2011.
8. F. Cannizzaro, J. De Los Rios, S. Caddemi, I. Caliò, S. Ilanko, On the use of a roving body with rotary inertia to locate cracks in beams, J. of sound and vibration. 425 (2018) 275-300.
9. S. Caddemi, I. Caliò, Exact reconstruction of multiple concentrated damages on beams, Acta mechanica. 225 (2014) 3137-3156.
10. A. Labib, D. Kennedy, C.A. Featherston, Crack localisation in frames using natural frequency degradations, Computers & structures. 157 (2015) 51-59.
11. S. Yadav, S.C Roy, J.N. Mahto, R.S. Prasad, Experimental investigation of crack in brass cantilever beam using natural frequency as basic criteria, International J. of scientific & engineering research. 5(2014) 447-454.
12. S.S. Kulkarni, U.C. Rajmane, P.J. Sawant, Crack detection in cantilever beam by frequency-based method, International J. of advanced research in science, engineering and technology. 3(2016) 1174-1177.
13. Priyadarshini, Identification of cracks in beams using vibrational analysis. MS thesis, National institute of technology. 2013.
14. K.H. Barad, D.S. Sharma, V. Vyas, Crack detection in cantilever beam by frequency-based method, Procedia engineering. 51 (2013) 770 – 775.
15. P.M Jagdale, M.A. Chakrabarti, Free vibration analysis of cracked beam, International J. of engineering research and applications 3 (2013) 1172-1176.
16. K.V. Bhinge, P.G. Karajagi, S.S. Kulkarni, Crack detection in cantilever beam by vibration techniques, International J. of Engineering research and applications. 3(2014) 80-86.
17. P. Yamuna, K. Sambasivarao, Vibration analysis of beam with varying crack location, International J. of engineering research and general science. 2(2014) 1008-1017.
18. D.N. Thatoi, J. Nanda, H.C. Das, D.R Parhi, Analysis of the dynamic response of a cracked beam structure, Applied mechanics and materials. 187 (2012) 58-62.
19. P.K. Jena, D.N. Thatoi, J. Nanda, D.R.K Parhi, Effect of damage parameters on vibration signatures of a cantilever beam. International conference on modeling, optimization and computing. 38 (2012) 3318 – 3330.
20. J. He, Z. Lu, Y. Liu, New method for concurrent dynamic analysis and fatigue damage prognosis of bridges, J. of bridge engineering. 17(2012) 396-408.
21. V.N. Rao, J.W. Eischen, Failure analysis of mixed mode crack growth in heavy duty truck frame rail, Case studies in engineering failure analysis. 5(2016) 67-74.
22. B. Dompierre, E. Wyart, M. Mesbah, M.F. Thirifay, Fatigue crack growth analysis on a rotor blade under forced response, Proceedings of ASME turbo expo, Texas, 2013, 1-9.
23. S. Rahmatalla, C. Schallhorn, Diagnosis of retrofit fatigue crack re-initiation and growth in steel-girder bridges for proactive repair and emergency planning, A cooperative research project. US department of transportation, 2014.
24. M. Sadek, J. Bergstrom, N. Hallback, C. Burman, Computation of and testing crack growth at 20 kHz load frequency, Procedia structural integrity. 2(2014) 1164–1172.
25. H. Cheng, H.B. Li, W. Zhang, Z.Q. Wu, B.R. Liu, Dynamic response analysis of an aircraft structure under thermal-acoustic loads, J. of Physics. 744 (2016) 1-8.

26. N. Zolghadri, M.W. Halling, P.J. Barr, N. Foust, Effects of temperature on bridge dynamic properties, Final Report, US department of transportation and research, 2015.
27. X. Lu, S. Li, H. Zhang, Y. Wang Y, X. Wang, Effect of thermal aging on the fatigue crack growth behavior of cast duplex stainless steels, International J. of minerals, metallurgy and materials. 22(2015) 1163-1170.
28. A.K. Syed, X. Zhang, J.E. Moffatt, M.E. Fitzpatrick, Effect of temperature and thermal cycling on fatigue crack growth in aluminum reinforced with GLARE bonded crack retarders, International J. of Fatigue. 98 (2017) 53-61.
29. M.A. Khan, S.Z. Khan, W. Sohail, H. Khan, M. Sohaib, S. Nisar, Mechanical fatigue in aluminum at elevated temperature and remaining life prediction based on natural frequency evolution, Fatigue and fracture of engineering materials and structure. 38(2015) 897-903.
30. M.A Khan, K.A. Khan, S.Z. Khan, S. Nisar, A. Starr, Fracture Life Estimation of Al-1050 Thin Beams using Empirical data and Numerical Approach, Insight. 60 (2018).
31. G. Ma. F. Chen. Yang, Modal analysis of a simply supported steel beam with cracks under temperature load, Shock and Vibration. 2017.
32. Y. Ma, G. Chen, Modal analysis of a rectangular variable cross-section beam with multiple cracks under different temperatures, J. of vibroengineering. 18 (2017) 2717-3424.
33. A. Mahi, E.A. Bedia, A. Tounsi, I. Mechab, An analytical method for temperature-dependent free vibration analysis of functionally graded beams with general boundary conditions, Composite structures. 92 (2010) 1977-1887.
34. Z. Wang, B. Liu, Y. Han, Free vibration frequency variation analysis of a cracked aluminum alloy beam under high temperatures, Journal of Harbin engineering university. 33 (2012) 320-324.
35. A. Gupta, N.K. Jain, R. Salhotra, Effect of thermal environment on vibration analysis of isotropic micro plate with inclined crack based on modified couple stress theory, 24th international congress on sound and vibration, 2017.
36. P.V. Joshi, N.K. Jain, G.D. Ramtekkar, G.S. Virdia, Vibration and buckling analysis of partially cracked thin orthotropic rectangular plates in thermal environment, Thin–Walled structures. 109 (2016) 143-158.
37. X. Zhao, Q.J. Hu, W. Crossley, C.C. Du, Y.H. Li, Analytical solutions for the coupled thermoelastic vibrations of the cracked Euler-Bernoulli beams by means of Green's functions. International J. of mechanical Sciences. 2017.
38. C. Comisu, N. Taranu, G. Boaca, M. Scutaru, Structural health monitoring system of bridges. Procedia engineering. 199 (2017) 2054–2059.
39. N.G. Shul'zhenko, B.F. Zaitsev, A.V. Asaenok, T.V. Protasova, Deformation and vibration-induced stress intensity of a high-temperature turbine rotor with a breathing transverse crack, Strength of materials. 49 (2017) 751-759.
40. P.J. O'Hara PJ, J. Hollkamp, Modeling fatigue crack propagation in a Ti-alloy at elevated temperature within a reduced-order model framework, Structures, structural dynamics, and materials conference California, USA. 2016.
41. B.A. Zai, M.A. Khan, K.A. Khan, A. Mansoor, M. Shahzad, The role of dynamic response parameters in damage prediction, Journal of mechanical science and engineering. 233 (2019) 4620–4636.
42. B.A, Zai, M.A. Khan, S. Z. Khan, M. Asif, K.A. Khan, A. Saquib, A. Mansoor, M. Shahzad, A. Mujtaba, Prediction of crack depth and fatigue life of an Acrylonitrile Butadiene Styrene cantilever beam using dynamic response, ASTM International J. of testing and evaluation. 48 (2019).
43. B.A, Zai, M.A. Khan, A. Mansoor, S. Z. Khan, K. A. Khan, Instant dynamic response measurements for crack monitoring in metallic beams, Insight. 61 (2019) 222-229.
44. A. Majid, Diagnosis of type location and size of cracks by using generalized differential quadrature and Rayleigh quotient methods, J. of theoretical and applied mechanics. 43 (2013) 61–70.
45. T. Irvine, Application of the Newton-Raphson method to vibration problems, 2 (2003) 1–16.
46. J.I. Rojas, D. Crespo, Modeling of the effect of temperature, frequency, and phase transformations on the viscoelastic properties of AA 7075-T6 and AA 2024-T3 aluminum alloys, metallurgical and materials transactions a physical metallurgy and materials science. 2012.
47. W.T. Thomson, Vibration theory and application 4th Ed. Prentice-Hall Inc. USA.
48. Y. Lee, Fatigue testing and analysis theory and practice, Elsevier Butterworth-Heinemann. UK, 2005.